

Dual beam multi-vane-loaded azimuthal supported angular log-periodic strip meander line slow-wave structure

CHEN Zi-Jun, WANG Zhan-Liang, LI Xin-Yi, HE Teng-Long, WANG He-Xin, GONG Hua-Rong, TANG Tao, DUAN Zhao-Yun, LU Zhi-Gang, HUANG Min-Zhi, GONG Yu-Bin*

(University of Electronic Science and Technology of China, Chengdu 610054, China)

Abstract: A bandwidth broadening and voltage reducing method for the azimuthal supported angular log-periodic strip meander line slow-wave structure has been proposed. By means of the vane-loaded technique to control the dispersion characteristics, the bandwidth of the azimuthal supported angular log-periodic strip meander line traveling-wave tube is expanded effectively. Through numerical simulation, it can be found that the 3 dB bandwidth of the structure without vane and with multi-vane loaded is 2.5 GHz and 3 GHz, respectively. The work voltage of the structure without vane and with multi-vane loaded is 5450 V and 4650 V, respectively. As the results shown, the bandwidth and work voltage of the angular log-periodic strip meander line slow-wave structure can be expanded and reduced by means of vane-loaded method.

Key words: vane-loaded, angular log-periodic, beam wave interaction, slow wave structure

PACS: 84.40.Fe

双注多翼片加载的角向夹持角度对数曲折线慢波结构

陈子君, 王战亮, 李新义, 何腾龙, 王禾欣, 巩华荣, 唐涛,
段兆云, 路志刚, 黄民智, 官玉彬*

(电子科技大学, 四川成都 610054)

摘要: 针对角向夹持的角度对数周期曲折线慢波结构, 提出了展宽其工作带宽、降低其工作电压的新方法. 通过翼片加载技术, 可以对慢波结构的色散特性进行修正, 从而使得其带宽得到有效展宽. 通过数值模拟仿真, 得到无翼片加载的慢波结构以及多翼片加载的慢波结构的 3 dB 带宽分别为 2.5 GHz、3 GHz, 工作电压分别为 5450 V、4650 V. 研究表明, 翼片加载结构可以有效降低角度对数周期曲折线慢波结构的工作电压, 以及展宽其工作带宽.

关键词: 翼片加载; 角度对数周期; 注波相互作用; 慢波结构

中图分类号: TN124 文献标识码: A

Introduction

As an important kind of vacuum electron device, traveling wave tubes (TWTs) are widely applied in radar, communication, electronic countermeasure and other electronic equipment. The helix TWTs are the most widely used devices in applications which require some important properties such as wide bandwidth, smooth RF

response, and high efficiency and so on. With the operating frequency of TWTs developing to millimeter-wave and THz range, the dimensions of the devices are reduced to micron-scale. The microfabrication technique and semiconductor silicon processing method have been adopted to the components processing^[1]. During this process, the planar slow wave structure has gradually developed, such as planar helix slow wave structure and angular log-periodic microstrip meander-line and so on.

Received date: 2018-12-13, **revised date:** 2019-05-29

收稿日期: 2018-12-13, **修回日期:** 2019-05-29

Foundation items: Supported by National Natural Science Foundation of China (61531010)

Biography: CHEN Zi-Jun (1996-), female, Hebei, China, master. Research area involves millimeter wave and terahertz wave vacuum electron devices. E-mail: chenzijunly@sina.com

* **Corresponding author:** E-mail: ybgong@uestc.edu.cn

The planar helix with straight-edge connections (PH-SEC) has been proposed^[2-3], and metal vanes have been shown to be effective in dispersion shaping of PH-SEC structure^[4].

The slow wave structure named angular log-periodic microstrip meander-line was proposed by Gong *et al*^[5]. And a lot of research works are explored to develop a miniature planar TWT with the microstrip meander line SWS, such as the optimal design of the SWS^[6], the EOS of fan-shaped radial divergent electron sheet beam with radial tunable PCM focusing system^[7] and so on. The microstrip structures have the properties of high efficiency, miniaturized dimensions, and easily to be integrated. In order to improve the performance in dissipating heat and resisting electron beam bombardment, the azimuthal supported angular log-periodic strip meander line SWS is proposed^[8]. The strip meander line is located in the middle of vacuum chamber and supported by two dielectric support sheets in azimuthal, as shown in Fig. 1. For expanding the bandwidth and reducing the voltage of this kind of slow wave structure mentioned above, the vanes are added and the multi-vane-loaded slow wave structure is presented in Fig. 2. As the simulation results shown, the 3-dB bandwidth of the structure is expanded 0.5 GHz and the work voltage is reduced 800 V by multi-vane loaded method.

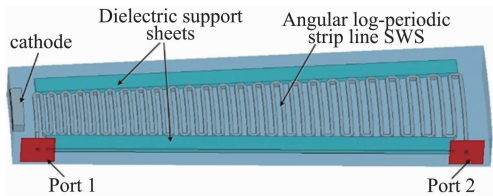


Fig. 1 Azimuthal supported angular log-periodic strip meander line SWS
图1 角向夹持角度对数曲折线慢波结构

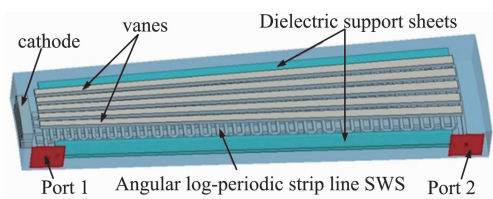


Fig. 2 Multi-vane-loaded azimuthal supported angular log-periodic strip meander line SWS
图2 多翼片加载的角向夹持角度对数曲折线慢波结构

1 The structure of the vanes

The metal vanes have been found very effective in dispersion shaping for the circular helix and the PH-SEC^[4]. By considering the structure of vanes, the radius of the vane is concentric with the circular helix in helix TWTs, and for the PH-SEC, the cross section of the vane is rectangle. As the angle log-periodic slow wave structure has the trend of divergence in radial direction,

the cross section of the vanes used in this kind of SWS is designed to be isosceles trapezoid. The formation of vanes is shown in Fig. 3. Two half-lines with an angle of θ_{vane} launch out from original point O , which is the center of the angular log-periodic meander-line, and they are on the symmetry of the middle axis. There are four intersections a, b, c and d which are formed by two half-lines and the first and the last segments of the angular log-periodic meander-line. Connecting four points forms the cross section of the vane in the $r-\theta$ plane. The single solid vane is formed by stretching the cross section a thickness of h_{vane} in the longitudinal direction, shown in Fig. 4(a). With O as the center, rotating the single vane an angle of θ_{rotate} with four times repeatedly is forming the multi-vane structure, as shown in Fig. 4(b). The number of the vanes is n , which is 5 in Fig. 4(b).

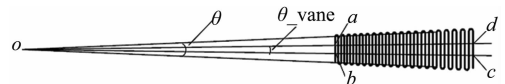


Fig. 3 The formation of the vane
图3 翼片形成示意图

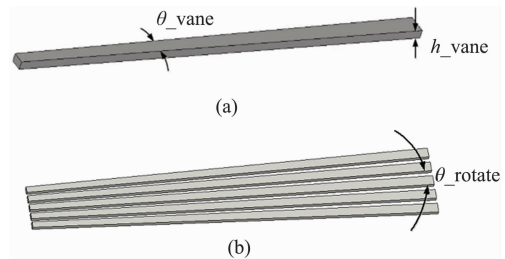


Fig. 4 The structure of (a) single vane, and (b) multi-vane
图4 (a)单翼片结构, (b)多翼片结构

2 The structure of the vane-loaded strip meander line SWS

The establish procedure of the angular log-periodic strip meander line is similar to the method mentioned in Ref. [6]. Figure 2 shows the multi-vane-loaded SWS. The material of the meander line and vanes is set as perfect electrically conducting (PEC), and the material of the dielectric support sheets is boron nitride (BN), with a relative dielectric constant $\epsilon_r = 4$ and a dielectric loss tangent $\tan\delta = 0.0005$. The relative position of the vanes and the angular log-periodic strip meander line of two methods are shown in Fig. 5 (vertical view and side view). The open angle of the vane is θ_{vane} , the thickness of the vane is h_{vane} , and the length of the vane is depended on the length of the strip meander line SWS. The height of vacuum chamber at one side of the SWS is h_{air} , and the gap between the vanes and SWS is the difference between h_{air} and h_{vane} .

The structure parameters we used are listed in Table 1. The parameters a, θ, b, w and t are initial radius, the open angle, growth rate, strip width, and strip thickness of the angular log-periodic strip meander line, re-

spectively. The dielectric support sheets' thickness and width are t_{sup} and w_{sup} . The length of dielectric support sheets is determined by the length of the strip SWS.

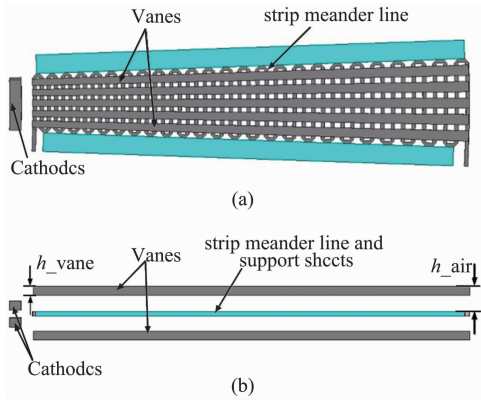


Fig. 5 The relative position of the vanes and the angular log-periodic strip meander line (a) vertical view of multi-vane loaded, and (b) side view of multi-vane loaded structure

图5 翼片与角度对数曲折线的相对位置(a)多翼片加载结构俯视图, (b)多翼片加载结构侧视图

Table 1 Parameters for the slow wave structure

表1 慢波结构参数

Parameters	values
a/mm	16
θ/deg	4
b	0.001 47
w/mm	0.075
t/mm	0.1
t_{sup}/mm	0.1
w_{sup}/mm	0.4
n (the number of vanes)	5
h_{vane}/mm	0.1
$\theta_{vane}(deg)$ of multi-vane	0.5
θ_{rotate}/deg	0.8
h_{air}/mm	0.4

3 Dispersion relation and interaction impedance of the slow wave structure

Angular log-periodic meander-line is not the standard periodic structure but a logarithmic periodic structure. The method of calculating the dispersion relation and interaction impedance of this kind of structures is proposed in Ref. [9]. According to this method, the phase velocity of the structure mentioned in this paper can be obtained from $v_p = \Delta r / \Delta t$, where Δr is the distance between the input and output ports, Δt is the time of signal propagating from input port to output port. By changing the frequency of the signal, the v_p varies with the frequency can be obtained, which means the dispersion relation curves can be obtained. As shown in Fig. 6, multi-vane loaded structure have lower normalized phase

velocity than the structure without vane, the normalized phase velocity of multi-vane structure is lower than 0.145, which can predict the lower work voltage. It shows that metal vanes are effective in reducing normalized phase velocity. This result can be interpreted as follows: for the vane-loaded structure, vanes are equivalent to the electrical boundary, and the distribution of the electric field is compressed towards slow wave line. While the distribution capacitance between vanes and slow wave line increases, the phase velocity will decrease. In summary, vane loaded technology is effective in dispersion control, which can get lower phase velocity.

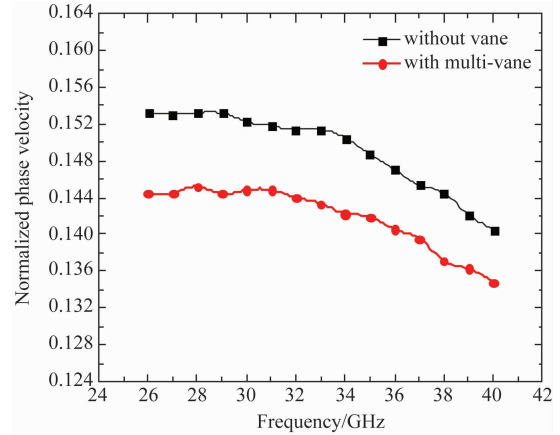


Fig. 6 Comparison of normalized phase velocity of multi-vane-loaded structure and no vane structure

图6 翼片加载结构与无翼片加载结构的归一化相速对比

In order to study on how the structure parameters of vanes effect on the dispersion relation, the variation of dispersion relation with the number of vanes, the thickness of vanes and the open angle of vanes are given in Fig. 7 (a-c).

Figure 7 (a) shows the variation of dispersion relation with the number of vanes when $h_{vane} = 0.1$ mm, $\theta_{vane} = 0.5^\circ$, the normalized phase velocity will decrease with the number of vanes increases. Figure 7 (b) shows the variation of dispersion relation with the thickness of vanes when $n = 5$, $\theta_{vane} = 0.5^\circ$, the normalized phase velocity will decrease with the thickness of vane increases. Figure 7 (c) shows the variation of dispersion relation with open angle of the vane when $n = 5$, $h_{vane} = 0.1$ mm. It can be seen that the open angle of vane has little influence on dispersion relation. Based on these results, the structure parameters of vanes are set as $n = 5$, $h_{vane} = 0.1$ mm and $\theta_{vane} = 0.5^\circ$.

The interaction impedance of these structures can be calculated by the formula $k_c = E_z^2 / 2\beta^2 P$. In Ref. [9], E_z and P can be obtained by setting the integral surface and integral lines, β can be calculated from $v_p = \omega / \beta$. The comparison of interaction impedance of multi-vane-loaded structures and no vane structure in the frequency range from 10 GHz to 40 GHz is shown in Fig. 8. It can be found out that the vanes have no significant influence on interaction impedance, and in the Ka-band which is from 26 GHz to 40 GHz, the interaction impedance of

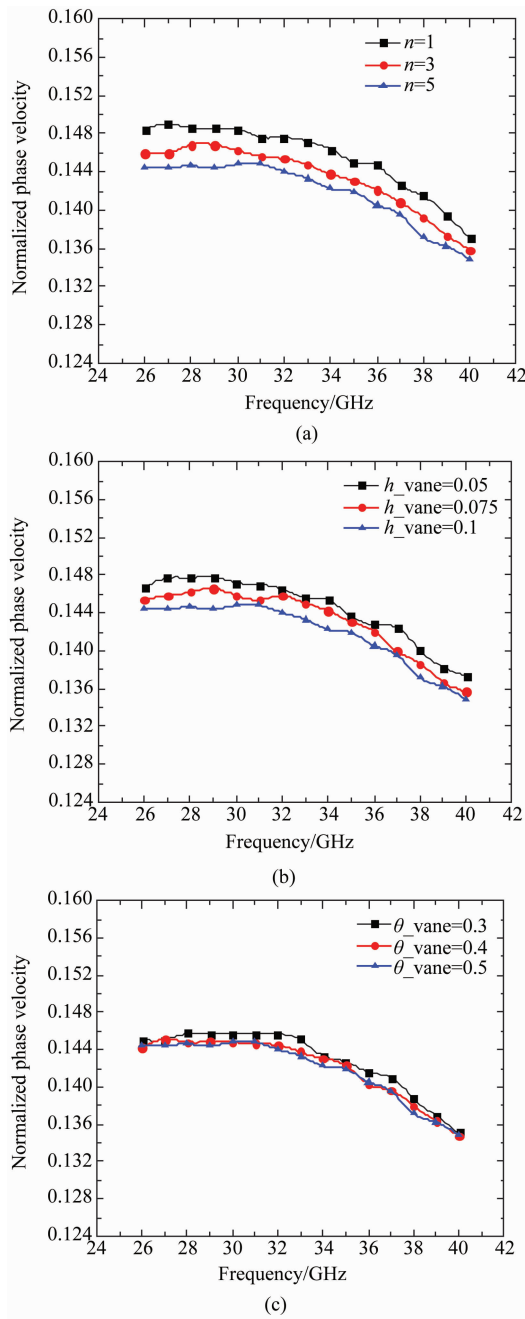


Fig. 7 Dispersion relation varies with (a) the number of vanes, (b) the thickness of vanes, and (c) the open angle of vanes
图7 色散曲线与(a)翼片个数,(b)翼片厚度,(c)翼片张角的关系

two structures approaches from 6.3Ω to 10.3Ω .

4 The transmission characteristics of vane-loaded slow wave structure

The transmission characteristics of SWS are usually expressed in S parameters. S_{11} is the reflection coefficient of port 1 when port 2 matches the load. S_{21} is the transmission coefficient of port 1 to port 2 when port 2 matches the load. The S parameters of the multi-vane loaded azimuthal supported angular log-periodic strip meander

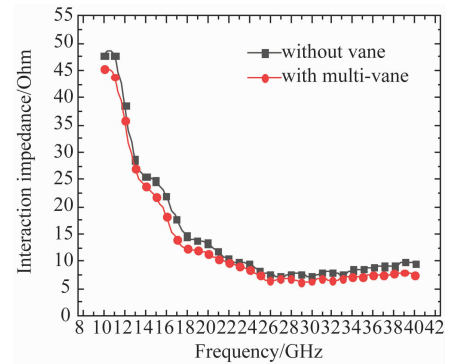


Fig. 8 Comparison of interaction impedance of multi-vane-loaded structure and no vane structure

图8 多翼片加载结构与无翼片结构的耦合阻抗对比

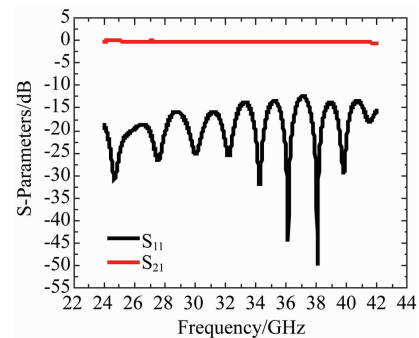


Fig. 9 S parameters of the vane-loaded SWS

图9 翼片加载结构的S参数

line SWS are calculated by CST and shown in Fig. 9. In the frequency range from 26 GHz to 40 GHz, S_{11} is less than -12 dB, and S_{21} is greater than -0.07 dB. The vanes have no significant influence on S parameters of the SWS mentioned in this paper.

5 Beam-wave interaction simulation results

To investigate the amplification performance of the multi-vane loaded azimuthal supported angular log-periodic strip meander line SWS, the beam-wave interactions of the models are simulated by PIC solver of CST Particle Studio. Two ideal cathodes are settled at the input side of the strip meander line with the thickness of 0.2 mm and on the symmetry of the strip meander line, both side at distance 0.02 mm over of the strip meander line surface, the position of the cathodes is shown in Fig. 5. Both of cathodes emit electron beam with dimensions $4^\circ \times 0.2$ mm propagated along the radial axis. The synchronous voltage of the electron beam is determined by the dispersion relation of the slow wave structure. As the phase velocity decreases, the required synchronous voltage decreases, which means the work voltage decreases. The work voltages of the structure without vane and multi-vane loaded structure are optimized to be 5 450 V and

4 650 V, respectively. Beam current is 0.3 A of each electron beam, and total beam current is 0.6 A.

In order to choose the appropriate input power, the saturation power curves of two structures are obtained, as shown in Fig. 10. The saturation output power of two structures are similar, close to 490 W, which makes a great agreement with the results of interaction impedance. As two structures have similar interaction impedance, the saturation power will be similar. The vane-loaded structure reaches saturation with input power of 12 W, and the structure without vanes reaches saturation with input power of 24 W. Considering the power available from solid-state devices, the input power of two structures are set as 5 W, and the beam-wave interaction results are obtained.

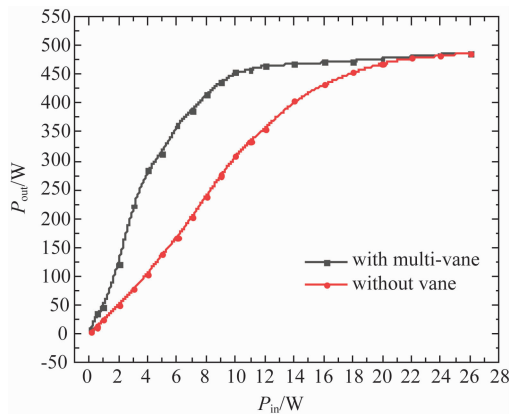


Fig. 10 The saturation output power curve of multi-vane loaded structure and no vane structure

图 10 多翼片加载结构与无翼片加载结构的饱和输出功率曲线

The beam-wave interaction results of multi-vane loaded structure at 38 GHz is shown in Figs. 11 (a-c). Figure 11(a) shows the electron bunching in the direction of motion, which is the necessary condition for beam-wave interaction. Figure 11(b) shows the electron beam kinetic energy variation along the radial distance. The kinetic energy of the electron beam is transferred to the electromagnetic field, so that the energy of electromagnetic field increases, the excitation signal is amplified. Figure 11(c) shows the frequency spectrum of the output signal obtained by Fourier transformation. It is relatively pure at 38 GHz.

With the input power of 5 W, the beam-wave interaction results of two kinds of structures are obtained. The comparison of gain of these structures are presented in Fig. 12. The gain of the structure without vane and structure with multi-vane loaded is 14.5 dB and 17.9 dB, respectively. The 3 dB bandwidth of structure without vane is 2.5 GHz, which is from 38 GHz to 40.5 GHz. The 3 dB bandwidth of structure with multi-vane loaded is broadened to 3 GHz from 38 GHz to 41 GHz.

As the simulation results shown, the multi-vane loaded SWS obtains better amplification performance. The voltage is 800 V lower than the structure without vane, which makes a great agreement with the dispersion relation. The maximum gain of multi-vane loaded SWS is 3.4 dB higher and the 3 dB bandwidth is 0.5 GHz broad-

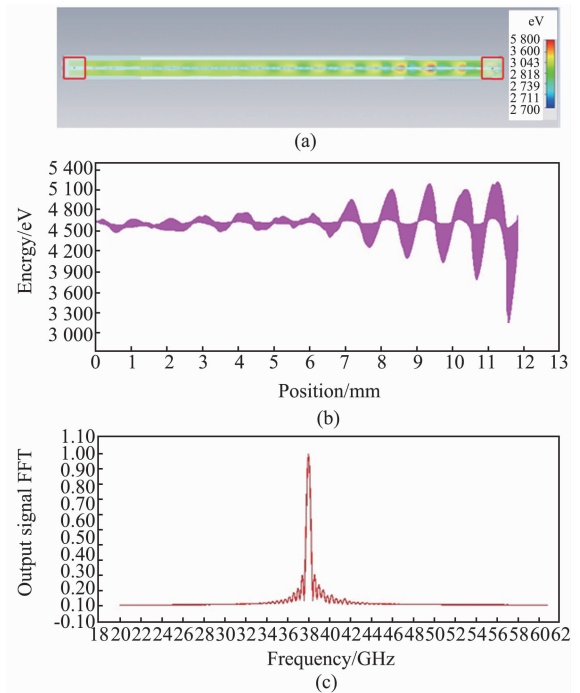


Fig. 11 (a) Electron bunching in the direction of motion, (b) electron beam kinetic energy variation along the radial distance, (c) frequency spectrum of the output signal

图 11 (a) 运动方向电子群聚情况, (b) 电子动能随径向距离的变化, (c) 输出信号频谱图

der than those of the structure without vane.

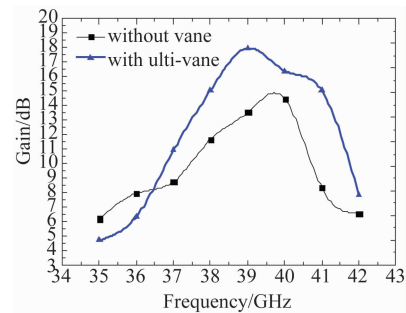


Fig. 12 Comparison of gain of multi-vane loaded structure and no vane structure

图 12 多翼片加载结构与无翼片加载结构增益对比

The beam-wave interaction results mentioned above are obtained based on lossless models. After that, the material of meander line and vanes is set as oxygen-free high-conductivity copper (OFHC) and the conductivity $\sigma = 5.8 \times 10^7$ S/m. The beam-wave interaction results are shown in Fig. 13. The output power of the lossy structure is slightly lower than the lossless structure.

6 Conclusion

The multi-vane-loaded azimuthal supported angular log-periodic strip meander line slow-wave structure is studied in this paper. Multi-vane loaded structure has

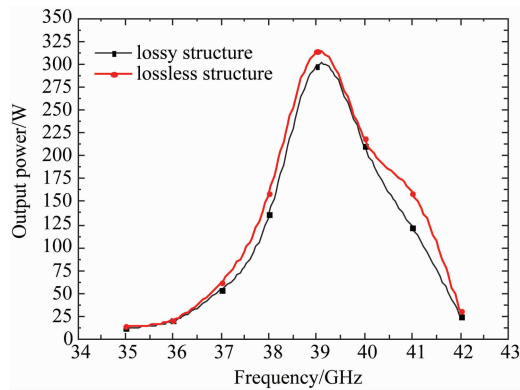


Fig. 13 Comparison of output power of lossless vane-loaded structure and lossy vane-loaded structure
图 13 考虑损耗的翼片加载结构与无损耗翼片加载结构的输出功率对比

lower normalized phase velocity than the structure without vane, and the vane has no significant influence on interaction impedance of SWS. According to the beam-wave interaction results, the multi-vane loaded SWS reaches saturation with lower input power than the structure without vanes. The work voltage of multi-vane loaded SWS is 4 650 V, which is 800 V lower than the voltage of SWS without vane. The 3-dB bandwidth of multi-vane loaded structure is 0.5 GHz broader than that of structure without vane. As the results shown, vane loading method can expand the bandwidth and reduce the work voltage of angular log-periodic strip meander line slow-wave structure.

References

- [1] Barker R J, Booske J H, Luhmann N C, *et al.* *Modern microwave and millimeter-wave power electronics* [M]. Piscataway, NJ, USA: IEEE Press, 2005.
- [2] Chua C, Aditya S, Shen Z. Planar helix with straight-edge connections in the presence of multilayer dielectric substrates [J]. *IEEE Trans. Electron Devices*, 2010, **57**(12):3451–3459.
- [3] Chua C, Aditya S, Tsai J M, *et al.* Microfabricated planar helical slow-wave structures based on straight-edge connections for THz vacuum electron devices[J]. *Int. J. Terahertz Sci. Technol.*, 2011, **4**(4): 208–229.
- [4] Swaminathan K, Zhao C, Chua C, *et al.* Vane-loaded planar helix slow-wave structure for application in broadband traveling-wave tubes [J]. *IEEE Transactions on electron devices*, 2015, **62**(3):1017–1023.
- [5] Wang S M, Gong Y B, Hou Y, *et al.* Study of a log-periodic slow wave structure for Ka-band radial sheet beam traveling wave tube[J]. *IEEE Trans. Plasma Sci.*, 2013, **41**(8): 2277–2282.
- [6] Li X Y, Wei Y Y, Wang Z L, *et al.* Study on phase velocity tapered microstrip angular log-periodic meander line travelling wave tube[J]. *IET MAP*, 2016, **10**(8):902–907.
- [7] Li X Y, Wang Z L, He T L, *et al.* Study on radial sheet beam electron optical system for miniature low-voltage traveling-wave tube[J]. *IEEE Transactions on Electron Devices*, 2017 **64**:3405–3412.
- [8] Li X Y, Wang Z L, Chen Z J, *et al.* Study on single radial sheet beam azimuthal support angular log periodic strip line travelling wave tube[C]. *International Vacuum Electronics Conference*, 2018, 135–136.
- [9] Wang S. Study of radial sheet electron beam travelling wave tube [D]. University of Electronic Science and Technology of China, 2013.